



# Chapter 1

## Introduction and Theoretical considerations

### Contents

<b>1. Introduction and Theoretical consideration</b>	
1.1 Introduction	2
1.1.1 Dilute magnetic alloys	3
1.2 Theoretical consideration	7
1.2.1 Dipole interactions	7
1.2.2 Spin Interactions	7
1.2.3 Heisenberg exchange interactions	8
1.2.4 Superexchange interactions	8
1.2.5 Double exchange interactions	9
1.2.6 Indirect exchange interactions	10
1.2.7 Disordered Magnetic systems	12
1.2.8 Hyperfine interactions in magnetic materials	13
1.3 Mossbauer parameters	15
1.3.1 Magnetic hyperfine splitting	15
1.3.2 Isomer shift	16
1.3.3 Second Order Doppler shift	20
1.3.4 Electric Quadrupole Splitting	21
1.4 Electric Field Gradients in Solids	25
1.5 Theory of defects in metals	27
1.5.1 Defects in metals	27
1.5.2 Method of defect production	27
1.5.3 Annealing procedure for the removal of defects	28
1.5.4 Identification of defects in materials	29
References	31

## **Introduction and Theoretical considerations**

### **1.1 Introduction**

Hyperfine interaction techniques are used to study microscopic properties of the materials. The interaction takes place between electromagnetic moments of nuclei and extranuclear fields, which results in the splitting or shifting of nuclear levels. These interactions give rise to changes in the energy levels of the order of  $10^{-7}$  to  $10^{-8}$  eV. So, compared to other conventional techniques, they are highly sensitive techniques to study local environmental effects like structural, electronic and dynamical properties of self-atoms and single impurities, inter-impurity and impurity-defect complexes on an atomic scale. Such studies are discussed and reported [1-5] widely in many journals. Even  $10^{13}$  probe ions can give us valuable information about the solid state properties. Of the various hyperfine techniques the Time Differential Perturbed Angular correlation (TDPAC) and Mossbauer spectroscopy are unique and versatile to study the materials.

Magnetic properties of the materials can also be studied microscopically to understand the actual mechanism of interactions between magnetic ions. The information such as long range & short range ordering, role of conduction electrons, spin fluctuations etc can be deduced from the hyperfine interaction parameters [6-8]. The high sensitivity to very low probe concentration in the matrix makes it an important tool to study the materials based on Dilute

Magnetic Alloys, where magnetic impurities are incorporated at very dilute concentration in the host lattice. The conventional bulk magnetization techniques fail to reveal the phenomena of interaction mechanisms in the dilute regime of such alloys.

### 1.1.1 Dilute Magnetic Alloys?

Dilute magnetic alloys are those materials in which a very small concentration of a magnetic ion is doped. They can be of two types based on their transport properties.

a) *Dilute magnetic metallic alloys* : In these alloys the transition metal impurities are doped into non magnetic metal hosts, such as CuMn [9], AuMn[10], CuFe [9]etc. Extensive studies have been reported in such canonical systems involving itinerant fermions and localized spin degrees of freedom. The low density of spins are perturbation on the Fermi liquid representing the nonmagnetic host metal. Hence depending on the concentrations they may be termed as dilute Kondo systems or amorphous magnetic systems with a spin-spin coupling mediated by the Fermi sea of conduction electrons which lead to spin glass behaviour [11]

b) *Dilute Magnetic Semiconductors (DMS)/Dilute Magnetic Semiconducting alloys (DMSA)* : DMS are composed of inert host semiconductors doped with both localized spins and carriers (electrons or holes) that are itinerant, or localized on a much longer length scale [12]. These materials exhibit a rich variety of novel physical phenomena and provide a unique combination of semiconducting and

magnetic properties. They are of great fundamental importance and technologically interesting because of the tunability of their physical properties by controlled doping of the concentration of impurities. These materials can be extensively used in opto-electronic and MRAM devices. With the use of these materials a new branch of electronics has emerged where the spin of the electrons is used in place of charge for information processing. It is known as SPINTRONICS.

DMS materials are made by alloying a compound semiconductor AB ( where A and B are elements of group (II-VI), (III-V), (IV-VI) or ( V-VI) of the periodic table) with magnetic ion impurities denoted by M. They are usually designated by the chemical formula  $A_{1-x}M_xB$  where x is concentration of magnetic ion. These semiconductors crystallize in the zinc blend or wurtzite structure and the element M enters the crystal substitutionally at cation sites[13]. Mostly these materials have shown the magnetic behavior at very low temperatures. But recent development in III-V based DMS have shown very good progress in raising the curie temperature to room temperature and above. For example magnetically doped ZnO, GaN, GaAs, GaSb and TiO<sub>2</sub> semiconductors showed curie temperatures above the room temperatures [14-16 ].

The Physical properties of transition metal ions in DMS are strongly influenced by the crystalline environment, they occur in different electronic configuration and charge states. Depending on the position of their energies within the band gap relative to fermi level, they can act as deep or shallow traps for electrons and

holes. The determination of electronic state as well as configuration and their dynamics is quite important for understanding the role of TM atoms in such isolated states. Magnetic order originates in the spin-spin exchange interaction between the 3d electrons of transition metal ions on the one hand and the band electrons on the other and the mechanism involved is called as sp-d exchange interaction. The magnetic behavior directly reflects the configuration of electrons in unfilled shell that is influenced by neighboring ions. Therefore the local magnetism of isolated transition metal ions in the host can be used to investigate and identify their electronic states.

The cause of ferromagnetism in III-V based DMS were well explained by Matsukara et.al [17] & Dietl. et. al. [18]. The mechanism was explained through carrier induced ferromagnetism at room temperature caused by exchange interaction between delocalized carriers and localized spins. However these carrier densities are brought into the systems by doping magnetic ion concentration which in turn should enhance the exchange interactions on increase of the concentration ( $M$ ). But it was observed that higher magnetic ion concentration may cause the formation of magnetic phases in the host material like MnN and MnAs [19] observed in GaMnN and GaMnAs systems.

However, in contrast if the dopant magnetic ion concentration is kept low and constant to avoid compound formation and the charge carrier densities can be brought about by varying the concentration of the anion in the semiconductor (B site in AB type), it will be still possible to keep the system in dilute limit and yet

may be possible to bring about ferromagnetism at room temperature. We have not come across in the literature anywhere such studies on the effect of variation of anion concentration in these systems. Most of the earlier studies have kept the A and B site concentration constant at the stoichiometric proportion of the compound . It will be interesting to study the effect of varying B site concentration in the II-VI, III-V, IV-VI or V-VI based systems. Hence instead of the stoichiometric compound a continuous alloy is to be formed between A and B with A as the base substance. Thus our present study differs in this respect where we have used the semimetal Sb as the base material and Se as the anion component. The general formula for our system was Fe in V-VI alloy  $Fe_xSb_{1-x}ySe_y$ . Fe concentration was kept low (0.002/0.008) and the charge carrier densities were brought in by varying the chalcogenide Se concentration. The details of the study are discussed in Chapter 3. Such systems we call Dilute Magnetic Semiconducting Alloys (DMSA).

Chapter 1 deals with the general introduction about dilute magnetic alloys and defects in metals. It also discusses the theoretical aspects of the concerned studies described in the thesis.

Chapter II discusses the experimental methodology and instrumentation associated with the study.

## 1.2. Theoretical Considerations

### Interaction of magnetic moments in solids:

#### 1.2.1 Dipole interactions

If the magnetic dipole moments  $\mu_1$  &  $\mu_2$ , separated by distance  $R$ , interact with each other, then classical interaction energy associated with it can be considered as,

$$U \sim \frac{\mu_1 \mu_2}{4\pi R^3}$$

On calculating the energy using standard values of  $R$ ,  $\mu_1$  &  $\mu_2$  shows that, the magnetic energy is smaller than thermal energy. But many materials exhibit magnetic ordering at Room temperature. Therefore, the classical approach of dipole interactions fails to explain the normal magnetic order mechanism.

#### 1.2.2 Quantum mechanical approach (spin interactions):

When the two magnetic atoms are close to each other, the electron densities of them begin to overlap and the spin states get modified. i.e. singlet state (spins antiparallel) and triplet states (spins parallel)[20]. However, the electrostatic electron-electron coulomb interaction energy associated will be same for both the states. But there is an additional contribution to the energy, which splits two states following the paulis exclusion principle. This is called as *exchange*

*interactions*. This is the primary magnetic interaction in solids and it is the simplest case of dipole interactions.

### 1.2.3 Heisenberg exchange interactions:

According to Heisenberg theory [21], the spin-spin exchange interaction in the solids with neighbouring ions can be represented as,

$$H = -\frac{1}{2} \sum_j J_j S_i S_j$$

where, J is the coupling constant which directly gives information about the difference in energy of spin states. The J can be of either sign. If J is positive, then the coupling is ferromagnetic (spins parallel) and if J is negative, then the interaction is antiferromagnetic (spins antiparallel).

Thus the two neighbouring atoms with direct overlap of electron densities in solids will produce magnetic interactions known to be direct exchange interactions.

### 1.2.4 Superexchange interactions:

The magnetic ions in solids may not interact via direct exchange, if they are displaced far apart from each other. Still the exchange interaction between magnetic cations in nonmagnetic anions could be possible, which is nomenclated as superexchange interactions. This superexchange is antiferromagnetic in nature. NiO, FeO, MnO are some of the examples of such interactions. The magnetic

moments of Ni/Mn/Fe interact with each other via intermediate anions of oxygen in such systems, thereby producing magnetic moments in solids.

### 1.2.5 Double exchange interactions.

Double exchange is a mechanism for spin coupling arising from electron delocalization. The term double exchange was originally introduced in 1951 by Clarence Zener to explain the magneto-conductive properties of mixed-valence solid, notably doped Mn perovskites. Zener proposed a mechanism for translocation of an electron from one Mn to another through an intervening  $O^{2-}$ . Because the oxygen p-orbitals are doubly occupied, the translocation had to proceed in two steps: the movement of an electron from oxygen to the "left" Mn followed by a transfer of a second electron from the "right" Mn into the (just) vacated oxygen orbital; hence the term double exchange.

Consider now a situation where one electron can delocalize over both iron sites of an  $Fe^{3+}Fe^{2+}$  dimer. Suppose the electron with the down spin is allowed to delocalize to the left. Because of the Pauli principle this electron can only delocalize into an orbital containing a spin-up electron. Intra-atomic exchange (Hund's rule) will maintain the parallel alignment of the spins on the left and the parallel alignment of the black spins on the right. Since delocalization of the extra electron does not involve spin flips (because the interaction leading to delocalization is spin-independent), the travelling electron forces the core spins of both metal sites into parallel alignment, resulting in nine unpaired spins. This

mechanism, also called spin-dependent delocalization, stabilizes an  $S = 9/2$  cluster ground state.

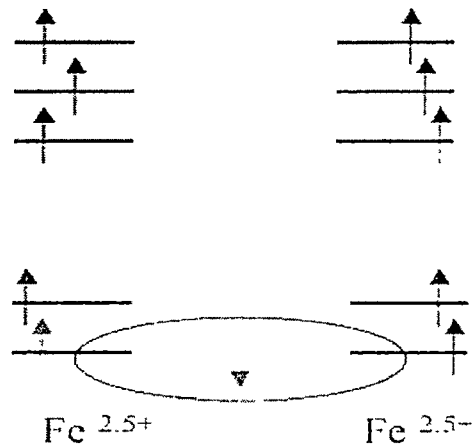


Fig 1.1 Double exchange between two Fe atom

The Hamiltonian yields

$$E = J S(S+1)/2 \pm B (S + 1/2)$$

where  $B$  describes the strength of the double exchange. For sufficiently large  $B$  the ground state of the mixed valence  $\text{Fe}^{2+} \text{Fe}^{3+}$  dimer will have  $S = 9/2$ .

#### 1.2.6 Indirect exchange interactions (RKKY interaction):

This is an important mechanism of magnetic coupling between localized moments in metals. It depends on the ability of conduction electrons to interact magnetically with local moments and to propagate between different magnetic sites. The theory of such conduction electron polarization and propagation was

first explained by Rudermann and Kittel [22] in 1954, which was extended to theory of s-f, s-d interactions by Kasuya and Yosida [23]. Thus the mechanism is known as RKKY mechanism. The spin polarization of conduction electrons is not only localized in the vicinity of the local moment but is oscillatory and long range ordered.

The basic idea of the mechanism is as follows.

The localized moments attract electrons with parallel spins, so that the net moment in the vicinity of the localized moment is enhanced. As the charge density is unchanged, there must then also be spatial regions where there is high density of spins with antiparallel alignment. Thus the wavelength of electrons will be in phase away from the moment. The result is that the localized moments set up an oscillatory spin density which becomes uniform at large distances.

The second localized moment will interact with this oscillatory spin density and hence will couple ferromagnetically or antiferromagnetically depending on the sign of spin density at that part. The strength of coupling is given by

$$J \sim \frac{1}{R^3} \cos(2K_F R) \text{ where } K_F \text{ is fermi wave vector.}$$

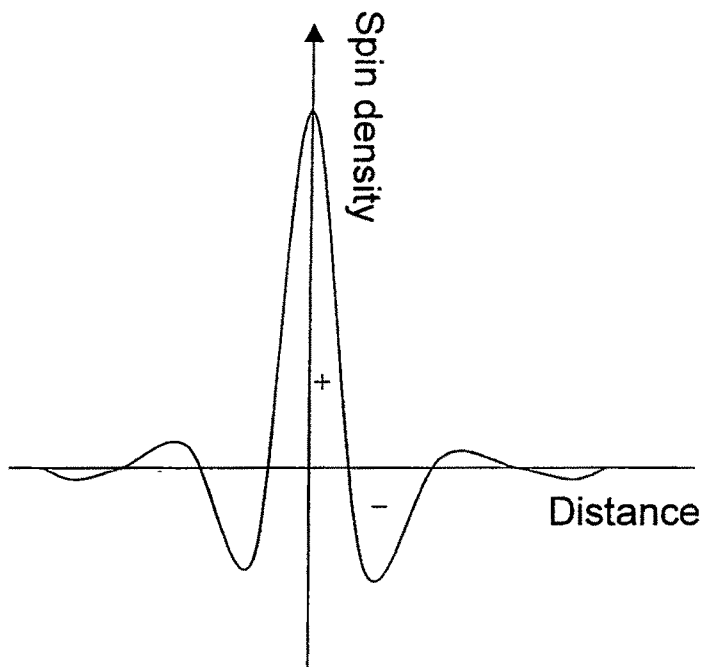


Fig. 1.2 RKKY interaction: the resultant distribution of conduction electron density

← ref.

The important feature of this interaction is that, it is long range ordering.

### 1.2.7 Disordered Magnetic systems (Spin Glass):

The random distribution of magnetic elements in alloys and compounds introduces strong disorder and deviation from a regular interaction pattern. The interaction between the magnetic constituents become random in size. This causes the appearance of new magnetic phases and phenomena.

?

Spin Glasses are one of the classes of disordered magnetic systems. The dilute magnetic alloys in which magnetic ions in very low concentrations are randomly dispersed in non magnetic host material shows such type of nature. This system

exhibits a freezing transition at a low temperature where the spins are aligned in fixed but random direction . Some of examples of spin glasses are  $\text{CuMn}$ ,  $\text{Eu}_{x}\text{Sr}_{1-x}\text{S}$ . The interactions in such systems are of RKKY type. The indication of cusp in the in-phase AC Susceptibility measurement [24] can reveal the spin glass nature of materials.

### 1.2.8 Hyperfine interactions in magnetic materials:

Hyperfine interactions are the interactions between atomic nuclei and the electromagnetic fields which surround them. It is a useful technique to investigate the interactions in solid materials from which the properties of extra nuclear electrons and about the solid state interatomic interactions can be deduced.

The hyperfine field ( $B_{\text{HF}}$ ) produced is predominantly caused by the net spin density at the nucleus due to the contribution of Conduction electron Polarization(CEP), Core polarization(CP) and overlap polarization (OP).

$$B_{\text{HF}} = B_{\text{CEP}} + B_{\text{CP}} + B_{\text{OP}}$$

The RKKY type of interaction can be the cause of conduction electron polarization. The core polarization occurs when a partly filled atomic d-shell is polarized by the conduction electrons of the host, which in turn polarizes the inner S- electron of the atom.

An electron  $j$  at point  $r_j$  and having angular orbital moment  $I$  and spin  $S$  induces on the nucleus at point  $r = 0$  a field which can be represented by the operator

$$H'_{hy} = -2\beta \left\{ \frac{I_j}{r_j^3} + \frac{3r_j(r_j S_j)}{r_j^5} - \frac{S_j}{r_j^3} + \frac{8\pi^2}{3} S_j(r_j) \right\}$$

Where  $\beta$  is the bohr magneton. The first term describes the field caused by orbital current due to electron movement. The second and third term describe fields caused by the magnetic dipole. The term with the delta function describes the Fermi contact part of the hyperfine interactions. The most important contribution is the Fermi contact term. It is the sum of the contribution of valence and core electrons. Core  $s$  states have very large charge densities at the nucleus and they give the main contribution to the hyperfine field, although they are only slightly polarized. Concerning the valence contribution, it is accepted that besides a relativistic treatment of the contact term, orbital contributions may be important. Usually, nuclear hyperfine fields are associated with local magnetic moments due to the observed proportionality relation between these two quantities.

The electron density effects at the nucleus and the interaction associated with it can be well observed by Mossbauer effect.

### 1.3 Mossbauer parameters:

The Magnetic hyperfine splitting, Isomer shift and the Electric quadrupole coupling are the three main Mossbauer parameters.

#### 1.3.1 Magnetic Hyperfine Splitting (Hyperfine Magnetic Fields-HMF).

Zeeman splitting of the nuclear levels is produced by the magnetic dipole interactions due to the presence of magnetic field (H) at the nucleus. The nuclear magnetic moment vector  $\mu$  which is collinear with I placed in a magnetic field H experiences a torque which tries to align the moment with the field. There is an energy associated with the degree of alignment and is given by

$$H_M = -g\mu_N \cdot H \cdot I_z$$

Where g is the nuclear lande factor,  $\mu_N$  is the nuclear magneton and the  $I_z$  is the z component of I in the direction of H.

The internal magnetic fields that exist in the materials like the ferromagnetic substances, have their origin in the following components.

The general expression for the magnetic field at the nucleus can be written as

$$H = H_0 - DM + 4/3\pi M + H_s + H_L + H_D$$

Where  $H_0$  is the magnetic field at the nucleus generated by an external magnet.  $H_s$  describes contact magnetic interactions between s-electron spin density and the nucleus (Fermi contact term).  $H_L$  is the contribution arising from the non zero

orbital magnetic moment and  $H_D$  arises from the dipolar interactions of the nucleus with spin moment of the atom. Fig 1.3 gives the schematic diagram of magnetic hyperfine splitting of  $^{57}\text{Fe}$ .

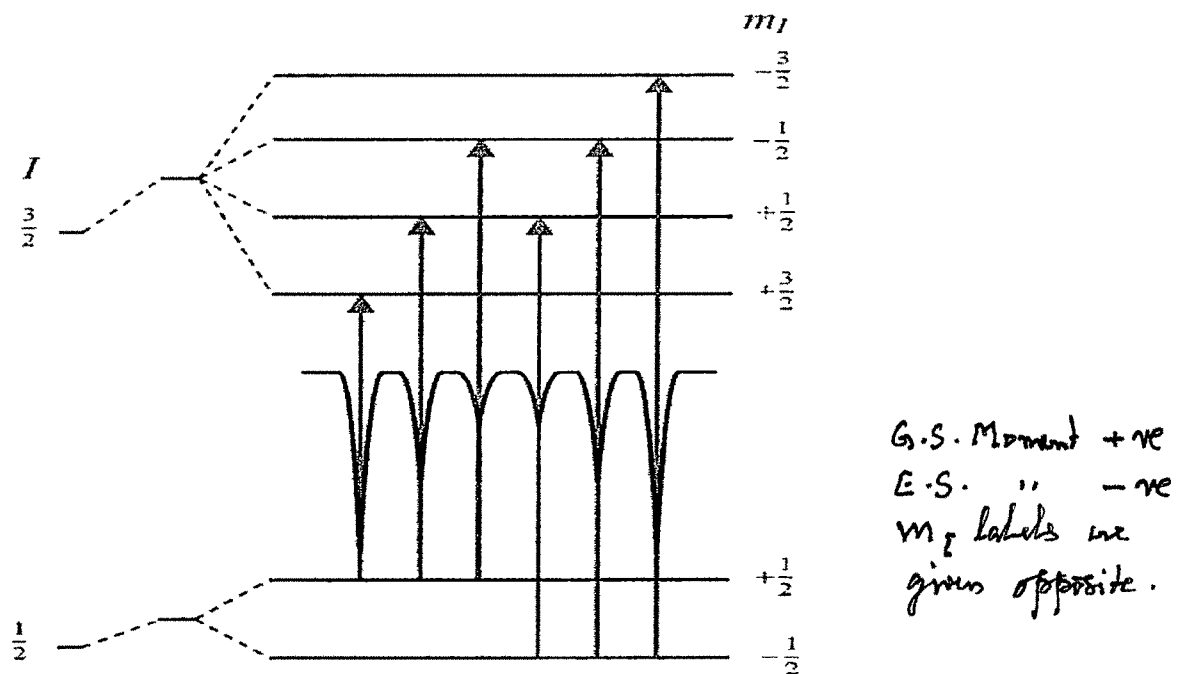


Fig 1.3. Schematic diagram of magnetic hyperfine splitting of  $\text{Fe}^{57}$ .

### 1.3.2 Isomer Shift

The electric monopole interaction between the electrons and the nucleus produces Isomer shift. The overlap of the electronic wavefunction with the nucleus via a Coulomb interaction affects the levels of the states[25]. In different materials with differing electronic properties a given type of nucleus can have a measurably different separation between the nuclear energy levels. The isomer shift involves a shift in nuclear energy levels resulting from differing electron

charge densities at the nucleus in the materials for the emitting and absorbing nuclei.

For an idealized atom consisting of a "point" nucleus with a Coulomb field, solving the Schrödinger equation gives ground state energy and some atomic (electronic) wavefunctions. The ground state energy level shifts ( $\delta E_s$ ) if the nucleus is an extended object of radius  $R$  and uniform charge density. In the first-order perturbation theory, this is obtained by letting the nuclear "perturbing Hamiltonian",  $H'$ , act upon the unperturbed ground state electron wavefunction,  $\psi^e$ .

$$\delta E_s = \langle \psi_s^e | H' | \psi_s^e \rangle \equiv \int \psi_s^{e*}(r) H'(r) \psi_s^e(r) d^3r \quad (1)$$

This gives the first-order energy shift for the ground state energy  $\delta E_e$ . One can calculate the energy of interaction between an extended Coulomb potential due to the nucleus with the electron cloud. The perturbing Hamiltonian is the difference between the point-like Coulomb potential that yielded the unperturbed wavefunctions,  $V_0$ , and the potential due to the nucleus modeled as a small uniformly-charged sphere,  $V$ .

$$H' = e(V - V_0) \quad (2)$$

$$V_0 = \frac{1}{4\pi\epsilon_0} \frac{Ze}{r} \quad (3)$$

and

$$\underline{V(r \leq R)} = \frac{Ze}{4\pi\epsilon_0} \frac{1}{R} \left( \frac{3}{2} - \frac{1}{2} \left( \frac{r}{R} \right)^2 \right) \quad (4)$$

The Hamiltonian contains no derivatives, so it doesn't really do anything to the wavefunction when it operates. The wavefunction of the electrons  $\psi_e(r)$  is taken to be constant over the range of the tiny nucleus, and is therefore taken out of the integral and replaced with  $|\psi_e(0)|^2$ , the probability density of the electrons at the origin. Evaluating the integral leads to

$$\delta E_\epsilon = \frac{1}{10\epsilon_0} Ze^2 R_n^2 |\psi_e(0)|^2 \quad (5)$$

A subscript n has been added to R to indicate that this is the radius of the n<sup>th</sup> state of the nucleus. Thus we see that for a given state n, the isomer shift depends upon the square of the "size" of the nucleus and upon the electron charge density at the location of the nucleus.  $R_n$  is not the same for all states. The shift of the energy levels for a given nuclear species depends upon the difference in electron densities between different materials. For a single material, the energy difference,  $\Delta E$ , between a ground state (0) and an excited state (1) would be

$$\Delta E = \frac{1}{10\epsilon_0} Ze^2 |\psi_e(0)|^2 (R_1^2 - R_0^2) \quad (6)$$

We must realize that  $|\psi_e(r)|^2$  or  $|\psi_e(0)|^2$  depends not only on a single atom's electrons, but also on the electrons of nearby atoms in the lattice of the given material.

Now if the emitter of a gamma ray and the absorber of that same gamma ray in the Mossbauer measurement have different electronic charge densities at the position of the nucleus, then we get a small shift in the difference of the energy levels:

This is called the isomer shift, and it causes the centroid of the Mossbauer spectrum to be displaced from zero relative velocity between emitter and absorber. Depending on whether the excited state has a larger or a smaller radius than the ground state, or whether the "s" electron densities ~~or~~ less or more the isomer shift will be either positive or negative. Fig 1.4 gives the schematic diagram of Isomer shift of  $^{57}\text{Fe}$ .

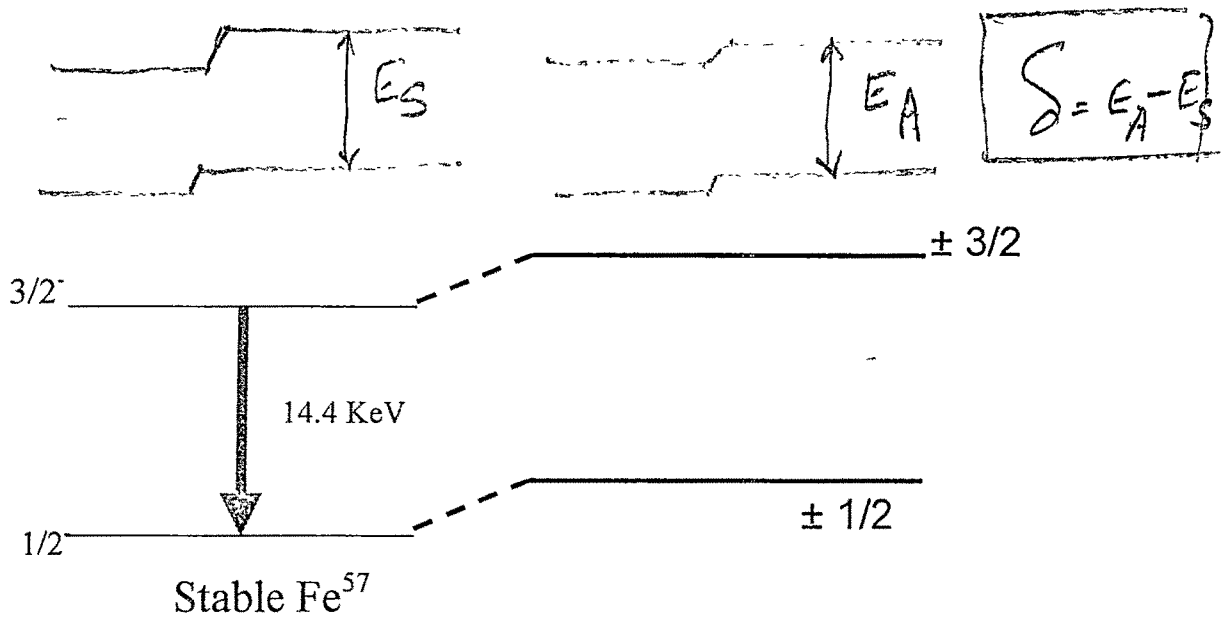


Fig. 1.4 Schematic diagram of Isomer shift .

1.3.3 Second Order Doppler shift

There is relativistic temperature dependent contribution to the isomer shift as pointed out by Pound and Rebka [ 26 ]. The relativistic equation for the Doppler effect on an emitted photon gives the observed frequency  $\nu'$ .

$$\nu' = \nu \left(1 - \frac{V}{C}\right) \left[1 - \frac{V^2}{C^2}\right]^{-1/2}$$

It is approximated as

$$\nu' \approx \nu \left(1 - \frac{V}{C}\right) \left(1 + \frac{V^2}{2C^2}\right)$$

where  $\nu$  is the frequency of stationary system. The velocity of the atoms vibrating on its lattice site in the direction of  $\gamma$ -ray will average to zero over the lifetime of the state. Hence only the second order term will contribute



$$EFG = -\nabla \nabla V.$$

? product of gradient operator to the three directional component electrical field, and is a tensor quantity. It is specified <sup>by the</sup> in three diagonal components of electric field as  $\partial^2 V / \partial x^2$ ,  $\partial^2 V / \partial y^2$  and  $\partial^2 V / \partial z^2$  (generally abbreviated as  $V_{xx}$ ,  $V_{yy}$  and  $V_{zz}$ ). <sup>in the Principal Axes System,</sup> These components obey the Laplace's equation i.e.

$$V_{xx} + V_{yy} + V_{zz} = 0 \quad \text{-----(1).}$$

As a result, there remains only two independent components, usually chosen arbitrary as  $V_{zz}$  and the asymmetry parameter  $\eta$ .

$$\eta = V_{xx} - V_{yy} / V_{zz} \quad \text{-----(2).}$$

The asymmetry parameter is useful in extracting many properties of electric field gradient (EFG).

For example, if the crystal has a fourfold axis, we can choose the arbitrary z axis as EFG tensor, a rotation by  $90^\circ$  produces no change in the crystal and can therefore produce no change in EFG.

The interaction Hamiltonian of electric quadrupole moment of nuclei and the EFG is as given below .

$$H = Q \cdot \nabla E \quad \text{-----(3).}$$

where  $Q_{ij} = \int \rho x_i x_j d^3x$ , or

The eigen values of quadrupole coupling is given as

$$E_Q = \frac{eqQ}{4I(2I-1)} [3m_l^2 - I(I+1)] \left[ 1 + \frac{\eta^2}{3} \right]^{1/2}$$

$$\uparrow = V_{zz}$$

The electric quadrupole interaction splits the nuclear excited state of  $Fe^{57}$  ( $I=3/2$ ) into sublevels having the energy eigen values as

$$E_Q = \frac{eqQ}{4} \left[ 1 + \frac{\eta^2}{3} \right]^{1/2}$$

The fundamental sources to EFG are the charges on distant ions and the electrons in incompletely filled shells. Distant ions contribute provided their symmetry is lower than cubic. Fig 1.5 and 1.6 give the schematic diagrams of Quadrupole splitting of  $I=3/2$  and  $5/2$  levels in axially symmetric field gradients.  $\Delta$  in  $I=3/2$  case represents the quadrupole splitting in the Mossbauer spectrum and  $\omega_1$ ,  $\omega_2 = 2\omega_1$  and  $\omega_3 = 3\omega_1$  in  $I=5/2$  case represent the interaction frequencies that can be detected in a TDPAC experiment.

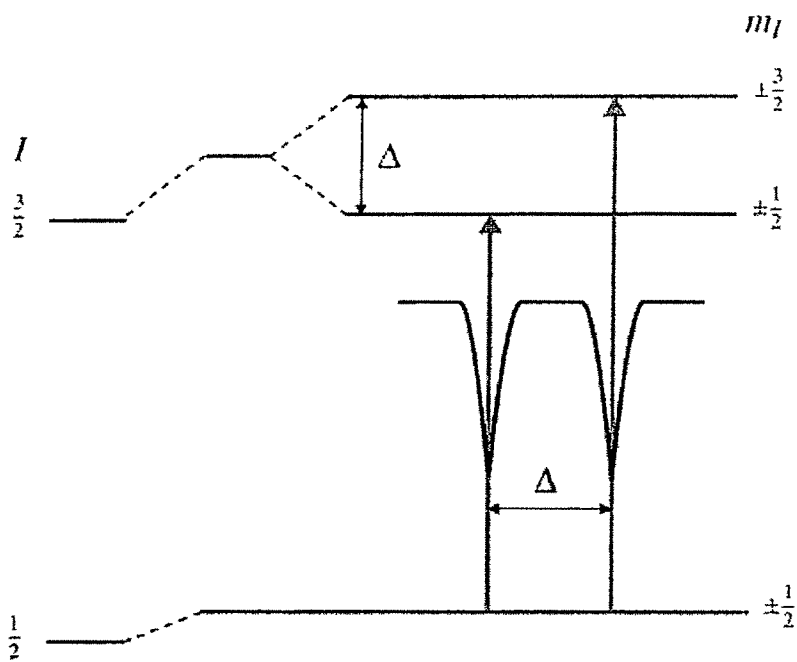


Fig. 1.5 Schematic diagram of quadrupole splitting

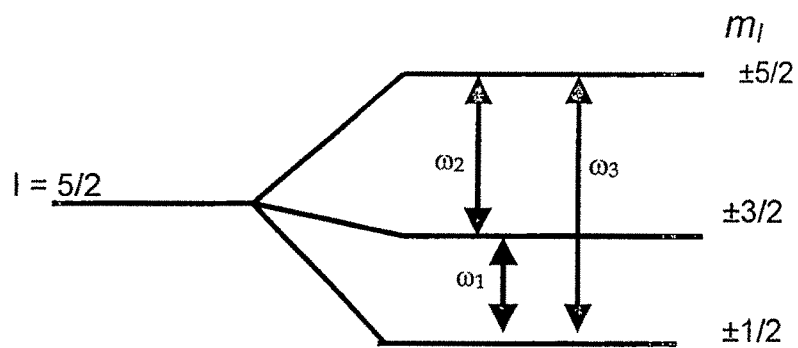


Fig. 1.6 Quadrupole splitting of spin  $I=5/2$  level in an axial symmetric electric field gradient

## 1.4 Electric Field Gradient in solids

It is quite well established that non spherical charge distribution in solids creates Electric Field Gradient (EFG). One can extract valuable information on the electronic structure of metals and alloys from the study of EFG. EFG being short ranged gives precise information about the local electronic distribution and its symmetry, the defects near probe and the local bonding nature. It has  $r^{-3}$  dependence [28].

However pure cubic metals with no defects present are spherically symmetric and hence do not possess EFG. But the non cubic metals possess asymmetric charge distribution due to contribution of lattice sites and conduction electron densities. The lattice field gradient ( $V_{zz}$  latt.) results from the non cubic arrangement of positively charged lattice ions while  $V_{zz}$  el. is caused by the negative charges of conduction electrons. The role of conduction electrons has been discussed by Watson et.al [29] and Das and Ray[30]. The lattice EFG can be estimated by the point charge lattice sum calculation. Its enhancement is taken into account by Sternheimer Antishielding factor  $(1-\gamma_a)$  [31].

The pioneering work done by Raghavan et.al [32] in metals have shown universal correlation between the contribution of lattice parameters  $[(1-\gamma)V_{zz}$  latt.] and conduction electrons  $V_{zz}$ el. According to this model  $V_{zz}$ el is approximately three times larger than  $[(1-\gamma)V_{zz}$ latt.] and has an opposite sign. It was expressed empirically as:

$e_{qel} = -Ke_{qlatt} (1-\gamma\alpha)$ , where K is the universal correlation.

It has also been observed that the temperature dependence of EFG in metals is observed to be following a  $T^{3/2}$  law[33]. The EFG in metals like Bi and Sb showed decreasing behaviour with increase in temperature, thereby indicating metallic nature. However several semimetals and semiconductors do not follow  $T^{3/2}$  law. The EFG in semiconductors like Te [34 ],  $Sb_2Te_3$  [35],  $In_2Te_3$  [36] and  $InBi$  [37 ] was found to be increasing steadily with temperature. But in high band gap semiconductors EFG is insensitive to temperature variation. This behaviour is observed in compounds like ZnO [38 ].

In Chapter 4, we have performed similar study to see the effect of temperature on dilute Fe doped in  $Sb_2Se_3$  semiconducting compound using Mossbauer Spectroscopic Technique.  $Sb_2Se_3$  is a V-VI group semiconducting compound with orthorhombic structure.  $Sb_2Se_3$  is reported to have a bandgap of 1.18 eV [39]. The effect of temperature on EFG of this compound is not reported previously.

## 1.5 Theory of defects in metals

### 1.5.1 Defects in metals

Defects in metals could be either extrinsic or intrinsic defects. The intrinsic defects like point defects (vacancies and interstitials) and extrinsic defects like impurities in the metals can be produced by various techniques or they are inherently present in some materials. The study of such defects, their production, migration, agglomeration and trapping are well studied in metals [40-42]. The variation of physical properties of the materials because of their electrically active nature in the matrix makes it important to study their dynamical behaviour.

### 1.5.2 Method of defect production

Lattice defects can be introduced in metals via 1) *irradiation*, 2) *quenching* and 3) *ion implantation* procedures.

1. Irradiation: The samples are bombarded with electrons or heavy ions. The defects produced are randomly distributed and may get trapped. They can produce structural defects like self interstitial atoms, vacancies and their agglomeration.
2. Quenching: The samples are cooled rapidly from high temperatures near the melting point. This effect can cause clustering in bound states or agglomeration.
3. Implantation: The energetic ions (especially probe atoms) are injected into target material using ion beam. The ion beam implantation can create

probe-defect complexes by forming bonds. Lot of work is reported on the study of the effect of implantation [43-47].

### 1.5.3 Annealing procedures for removal of defects:

Isochronal annealing procedure as discussed by Pfeiler et. al. [48] is usually employed for identification of defect formation. In this procedure, the samples are heated to a range of annealing temperatures for a short time (about 10 min) and then remeasured at the temperatures at which defects were first introduced. The probe-defect complexes gets modified, as the defects become mobile at their annealing stages.

Defects recovery model in metals [48] :

Annealing stages	Temperature (expressed as fraction of melting point)	Description
I <sub>A</sub> -I <sub>D</sub>	0.02	Recombination of close interstitials-vacancy pairs
I <sub>E</sub>	0.025	Free migration of interstitials followed by formation of interstitial clusters.
II	0.02 - 0.2	Growth of interstitial clusters
III	0.12- 0.2	Free migration of mono or divacancies leading to annihilation at interstitial clusters.
IV	0.12-0.4	Growth of vacancy clusters
V	0.5	Dissociation of remaining interstitials and vacancy clusters, removal of most of the remaining defects

#### 1.5.4 Identification of defects in materials:

Usually conventional techniques [49] are used for the detection of defects in metals. But they are not sensitive to the low probe-defect concentration in the material. Instead, the microscopic local probe techniques like  $\gamma$ - $\gamma$  perturbed angular correlation and Mossbauer spectroscopy are highly sensitive to even impurity concentration of  $10^{13} \text{ cm}^{-3}$  in the matrix.

**Table 1. Various techniques used for investigation of defects produced [48]:**

Methods	Application to	Limitations
Mechanical relaxation	Vacancies and interstitials	Requires single crystals
Diffuse X ray scattering	Mainly interstitials	Requires single crystals
Electron microscopy	Vacancy, interstitials, clusters, loops	Applicable to large defects
Field ion microscopy	Vacancies and interstitials	Requires high melting point
Channeling	Lattice location of defects	Requires single crystals
Positron annihilation	Vacancies and small clusters	Not sensitive to defect geometry.
Hyperfine interaction	Impurity-defect bound states for small defects	Provides unique "flags" of defects, quantitative interpretation of data is difficult

Through table 1 one observes that the type of microscopic complexes between probe-impurity can only be detected by Hyperfine interaction technique. The Electric Field Gradients associated with each complex determines specific structures of local environment around the probe.

The first attempt to study such defects in materials using PAC technique was made by Kaufmann et. al. [50] in the year 1977. After which numerous studies in different materials were done using same techniques [43-47]. In most of the studies annealing procedure was employed for identification of type of defects and its nature.

For e.g. the annealing procedure of radiation damage produced in chalcopyrites studied by S.Unterricker et. al. [51] have shown interesting results. The reports explains the removal of amorphization caused by radiation damage through isochronal annealing steps. The prominent sharp quadrupole frequency observed after annealing procedures were interpreted as the probes diffusing more towards chalcopyrite environment in the system.

We report in Chapter 5 similar studies done in radiation induced damage effects in Rhodium (Rh) metal using TDPAC technique. . Isochronal annealing for 10 min was done at 300, 1073 and 1473 K temperatures. As irradiated sample showed two Quadrupole interaction frequencies 1150 MHz and 93 MHz. The slow frequency disappeared at room temperature annealing which was assigned to In trapped at a vacancy created by radiation damage, while the higher frequency remained upto high temperatures and was attributed to In trapped at Rh-C complexes in the Rh matrix. ?

Chapter 6 gives the summary and future scope of the studies.

## References:

1. E.Recknagel, G.Schatz, Th Witchert, Hyperfine interactions of Radioactive Nuclei .ed. J. Christiansen, Topic Current Phys., Vol 31 (springer, Berlin, Heidelberg 1983)p.133.
2. M. Forker, R.J.Vianden, Magnetic Resonance Rev. 7. 275 (1983).
3. G. Marx and R.Vianden, Hyperfine interactions, 93 (2996) 211-219
4. R.Vianden, Nuclear Physics Applications on Material Science eds. E.Recknagel and J.C.Soares NATO ASI E 144 (1987) 239
5. D. F.Wirth, Rep. Prog. Phys. 62 (1999) 527-597.
6. J. Crangle, The Magnetic Properties of Solids, ed. By Edward Arnold (publishers) limited, 1977
7. M. F. Thomas & C.E.Johnson, Mossbuaer spectroscopy of magnetic solids.  
P143 *Publisher?*
8. D. L.Williamson, L. Niesen, G.Weyer, R.Sielemann and G. Langouche, Hyperfine interaction of defects in semiconductors, ed. By G.Langouche, Elsevier, Netherlands (1992)
9. A.K.Nigam and A.K.Majumdar, J. Appl. Phys. 50 1712 Year?
10. A. Mookerji, J.Phys. F, Met. Phys. 10 (1980) 1559-1566
11. J.A.Mydosh, Spin Glasses: An Experimental introduction (Taylor and Francis, London,1993)
12. R.N.Bhatt, M Berciu, M.Kennet, X.Wan, J. Supperconductivity, 15 (2002)71.

13. M. Jain, Dilute Magnetic Semiconductos ??
14. K. Ueda, H.Tabata and T.Kawai, Appl.Phys. Lett. 79 (2001) 988
15. M.L.Reed, E.L.Masry, H.H.Stadelmaier, M.K.Ritums, M.J.Reed,  
C.A.Parker, J.C.Roberts and S.M.Bedair, Appl. Phys. Lett 79 (2001)3473.
16. Y Matsumoto et.al. Science 291 (2001) 854 .
17. F.Matsukura, H.Ohno, A.Shen and Y.Sugawara, Phys. Rev. B 57, R2037  
(1998).
18. T.Dietl, A.Haury and Y. Merle d'Aubigny, Phys. Rev. B 55, R3347 (1997).
19. F. Matsukura, E. Abe, H. Ohno, J. Appl. Phys. 87 (9) (2000)  
6442.
20. D. Jiles, Introduction to Magnetism and Magnetic materials, ed. By  
Chapmann and Hall, London (1994)
21. W. Heisenberg, Z. Phys., 49(1928)619.
22. Ruderman M A and Kittel C 1954 Phys. Rec. 96 99
23. Yosida K 1957 Phys. Rev. 106 893
24. J. A. Mydosh, J. Magn. Magn. Mater. 157/158, 606 (1996).
25. G.K.Shenoy and F.E.Wagner, " Mossbauer Isomer Shifts", North Holland,  
Amsterdam, 1975.
26. R.V.Pound and G.A.Rebka, Phys.Rev.Lett., 4 (1960), 341
27. W.L.Gettys, J.G.Stevens, In C.R.C. Handbook of Spectroscopy, Vol III. Page?
28. O. Kanert and M. Mehring, " NMR -Basic Principles and Progress, 3 Ed. P.  
Diehl, E. Fluckand, R.Kosfeld (Springer, Berlin)1971.

29. R.E.Watson, A.C.Gossard, Y.Yafet, *Phy.Rev* 140 (1965) 375
30. K.C.Das, D.K.Ray, *Phys. Rev.*187(1969) 777
31. R.M.Sternheimer, H.M.Foley, *Phy. Rev.*, 92(1952) 1460.
32. P. Raghavan, E.N.Kaufmann, R.S.Raghavan, *Phys.Rev.Lett.* 34 (1975) 1280.
33. J. Christiansen et.al. *Z.Phys.* B24 (1976) 177.
34. H. Barfuss,G.Bohnlein, H. Hohenstein, A.Reiner, *Z.Phys.* B 45 (1982)193
35. H. Barfuss, Thesis Erlangen, 1984
36. H. Wolf, D.Forkel, Private Communication
37. D.Forkel, W Recknegal, M. Iwatschenko, R.Ketel, W.Withuhn, *Hyp.Int.*  
15/16 (1983) 821.
38. G. Pal, Thesis. 1999
39. I.S.Grigoriev, E.Z.Meilikhow, CRC Hand book of Physical Quantities. *Page!*
40. A. Seeger, D.Schumacher, W.Schilling, J.Diehl, *Vacancies and Interstitials  
in metals* (North Holland, Amsterdam) 1970
41. M.T.Robinson and F.W.Young, *Fundamental Aspects of Radiation damage  
in metals*, Springfield, 1976
42. *Properties of Atomic defects in metals*, ed. By N.L.Peterson and R.W.Siegel,  
NorthHolland, 1978.
43. J.C.Austin, W.Hughes, B.Patnaik,R.Triboulet, M.Swanson, *J. Appl.Phys.*  
86(1999) 3576
44. A. Hoffmann,, A. Willmeroth and R.Vianden, *Z.Phys.* B 62(1986)335.
45. E.Lohmann, Th.Schafer, M.Weheimer, R.Vianden, *Mat. Sci.Forum* 143-

147(1994)1155

46. W.Withuhn, NIM-B. B 63 (1992) 209-216.
47. D.Forkel Wirth, NIM-B 126(1997) 396-405.
48. F.Pleiter, C.Hohenemser,Phy.Rev. B 25(1982)106
49. J.M.Spaeth, J.R.Niklas, R.Bartram, Structural analysis of point defects in solids, solid State Sciences 43, (Springer, Berlin 1992)
50. E.N.Kaufmann, R.Kalish, R.A.Naumann,S.Lis, J.Appl.Phys. 48(1977) 3332.
51. S.Unterricker, T.Butz and S.Saibene, NIM-B 63(1992) 236-239.